ADVANCED FUNCTIONAL MATERIALS
www.afm-journal.de

Chemically Stable, Strongly Adhesive Sealant Patch for Intestinal Anastomotic Leakage Prevention

Alexandre H. C. Anthis, Xueqian Hu, Martin T. Matter, Anna L. Neuer, Kongchang Wei, Andrea A. Schlegel, Fabian H.L. Starsich, and Inge K. Herrmann**

Intestinal anastomotic leaking, which involves the discharge of chemically aggressive, non-sterile fluids into the abdomen, remains one of the most dreaded postoperative complications of abdominal surgery. Depending on the site and the patient condition, incidence ranging between 4% and 21% and mortality rates up to 27% are reported. Currently available surgical sealants only poorly address the issue, especially since most commonly used fibrin glues fail due to insufficient adhesion and chemical instability. Here, a chemically highly resistive, leak-tight, and mucoadhesive hydrogel sealant, which is grafted on the surface of the intestinal wall using a mutually interpenetrating network that traverses hydrogel and tissue is presented. In contrast to clinically used fibrin-based sealants (including Tachosil), the developed adhesive poly(acrylamide-methyl acrylate-acrylic acid) patch does not degrade and exhibits strong tissue adhesion even when exposed to intestinal fluid. The biocompatible hydrogel patch effectively seals anastomotic leaks in ex vivo intestinal models, greatly surpassing commercial sealants (time to patch-failure >24 h compared to 5 min for commonly used Tachosil). Importantly, the developed adhesive patch paves the way for the application of both mechanically and chemically robust sealants suitable for the treatment and prevention of intestinal leaks.

1. Introduction

As the world population is aging due to increasing life expectancy, chronic diseases play an ever-important role in the expenditures of patients and healthcare systems.[1] Of those, colorectal cancers, bowel ischemia, and inflammatory diseases such as Crohn's disease or ulcerative colitis, often require invasive surgical procedures. Typically, these interventions consist of removing or circumventing diseased tissue and connecting the remaining healthy tissue extremities by standard suturing or stapling. Such abdominal organ anastomoses are necessary and lifesaving, however, can be accompanied by dreaded complications, which lead to longer hospitalization and recovery times of patients.[2] Leaks of the intestinal tract, containing digestive and microbially rich intestinal fluid are especially feared, as they can lead to peritonitis, sepsis, and ultimately death.[3] Typically, leakage incident rates may vary between 4% and 21%, greatly depending on the patient's condition (sarcopenia level among others[4]) as well as the surgeons experience.[5] Patients that suffer anastomotic leaks have reported mortalities that can range between 13% and 27%.[6] In the highly feared scenario of septic peritonitis, mortality rates can reach values as high as 50%.[7]

Material science and engineering have over the years attempted to develop materials, that can adhere to all types of tissues as well as assist the healing process.[8–10] Of these, focus was first put on multipurpose surgical adhesives as well as on suture supports.[11] Cyanoacrylates were among the first ones to be employed for sealing purposes but surgeons gradually abstained from their use in percutaneous operations,[12] due to their innate toxicity and mechanical incompatibility with soft tissues.[13,14] Later on, adhesives based on synthetic polymers, such as polyurethanes, polyethylene glycols, and polyesters were developed. They were proposed as surgical materials for applications ranging from preventing air leaks in thoracic surgeries to suture supports in reconstructive operations, due to their resistance to fatigue and tailorable degradability.[15] Importantly, also natural polymers such as fibrin, collagen, and cross-linked albumin made their dent on the market of surgical adhesives thanks to their biocompatible and degradable properties. Such natural polymer-based adhesives have since found a broad application spectrum in various conditions,[16] however, their clinical benefit is variable and highly dependent on the tissue characteristics and clinical condition.[17]

A. H. C. Anthis, X. Hu, Dr. M. T. Matter, A. L. Neuer, Dr. F. H. L. Starsich, Prof. I. K. Herrmann
Laboratory for Particles Biology Interactions
Department Materials Meet Life
Swiss Federal Laboratories for Materials Science and Technology (Empa)
Lerchenfeldstrasse 5, St. Gallen CH-9014, Switzerland
E-mail: tino.matter@empa.ch; inge.herrmann@empa.ch, ingeh@ethz.ch

A. H. C. Anthis, Dr. M. T. Matter, A. L. Neuer, Dr. F. H. L. Starsich, Prof. I. K. Herrmann
Nanoparticle Systems Engineering Laboratory
Department of Mechanical and Process Engineering
ETH Zurich
Sonneggstrasse 3, Zurich CH-8092, Switzerland

Dr. K. Wei
Laboratory for Biomimetic Membranes and Textiles
Swiss Federal Laboratories for Materials Science and Technology (Empa)
Lerchenfeldstrasse 5, St. Gallen CH-9014, Switzerland

Dr. A. A. Schlegel
Liver Unit
Queen Elizabeth University Hospital Birmingham
Mindelsohn Way, Birmingham B15 2WB, UK

The ORCID identification number(s) for the author(s) of this article can be found under https://doi.org/10.1002/adfm.202007099.

DOI: 10.1002/adfm.202007099

With an increasing understanding of the underlying pathophysiology of tissues and conditions requiring surgical adhesives as well as the healing impairment induced by surgical procedures, a push for surgical materials specifically designed for a given tissue has been sparked.[15] In the case of intestinal anastomotic material supports, commonly and broadly employed products are fibrin-based Tachosil or Tisseel. However, these materials have been predominantly used to assist the healing process at the anastomotic sites while attention has rarely been placed on the distinct requirements to seal intestinal anastomosis leaks (anastomotic leak reduction was only assumed[18]). As a result, the long-term sealant properties, the interaction of the surgical materials with the intestinal fluid itself as well as the leak prevention or absorbing properties of those materials have not been evaluated.

Thus, in line with the recent push for highly tailored solutions for specific organs and conditions,[15] we present a chemically stable, leak-tight, mucoadhesive hydrogel sealant, which can be grafted to intestinal tissue via a mutually interpenetrating network that traverses simultaneously tissue and hydrogel patch. Our formulated hydrogel and its mutually interpenetrating network are composed of copolymerized acrylamide, acrylic acid, methyl acrylate and bis-acrylamide, each of these components selected respectively for their network forming ability,[19,20] mucoadhesive character,[21] hydrophobic nature,[22] and stability toward degradation.[23] These components operating in synergy serve the purpose of differential swelling in different physiological fluids as well as non-digestibility by intestinal fluid enzymes. Taken together, these assets distinguish the developed adhesive patch from recently published multipurpose intraperitoneal chitosan patches,[24] alginate/polyacrylamide bridging polymer-based systems,[9,25] and the routinely used fibrin-based sealant Tachosil. The hydrogel patch was developed with the goal of sealing as well as countering anastomotic leaks. To this end, the patch performance was investigated in two different ex vivo scenarios designed to enable quantitative assessment and benchmarking against conventional fibrin-based materials. The assessment of its performance under chemically harsh digestive conditions and the comparison to clinically used adhesives are important steps in the materials design and development process.

2. Results and Discussion

Figure 1 depicts a schematic of the synthesis steps followed for the preparation and application of the proposed hydrogel patches. Poly(acrylamide-methyl acrylate-acrylic acid) P(AAm-MA-AA) hydrogels were prepared by radical polymerization of acrylamide, methyl acrylate, acrylic acid, and bis-acrylamide (molar ratio of AAm/MA/AA/mBAA: $1/0.8/2/5\times10^{-3}$) using low dose UV light (9 J cm^{-2}). The synthesis yielded a gel content[26] coinciding with the expected theoretical gel and water ratio, pointing to a complete polymerization (see Table S1, Supporting Information). The chemical structure was also characterized by nuclear magnetic resonance spectroscopy (see Figure S1, Supporting Information). Materials were chosen in order to maximize mucoadhesion (see Figure S2, Supporting Information) while maintaining mechanical integrity during prolonged exposure to biological fluids (e.g., PBS, bile and intestinal fluid [see Figure S3 and Table S2, Supporting Information]). Furthermore, the utilized components stand out due to their comparably low material costs (i.e., 75–120$ per metric ton[27]) and production scalability,[28] which is a frequently overlooked pre-requisite for a successful clinical translation.

After the initial polymerization step, two distinct approaches were investigated for the tissue-application of the proposed

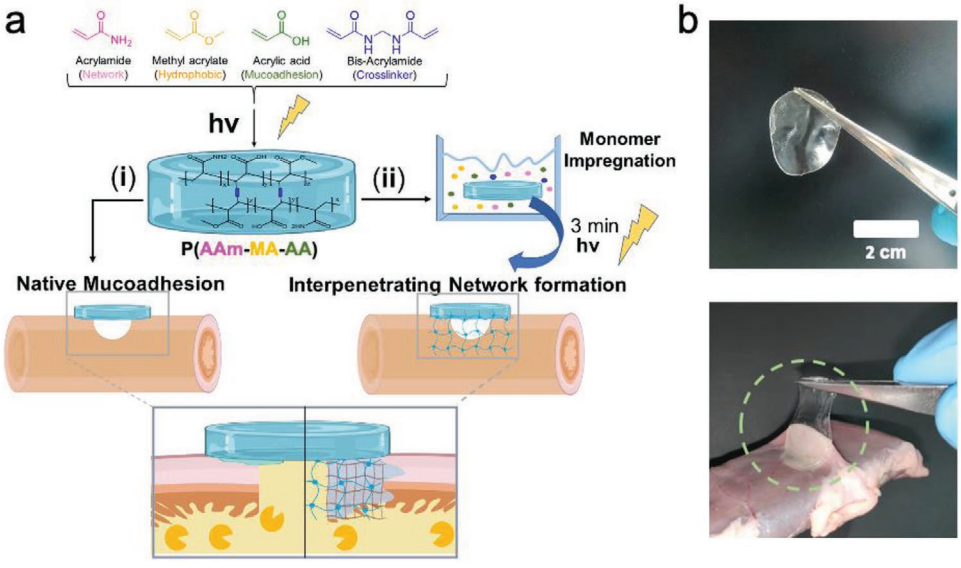

Figure 1. a) Formulation and formation of the P(AAm-MA-AA) hydrogel patch using bis-acrylamide as a crosslinker. Application as i) "ex situ" hydrogel system and attachment based on mucoadhesion, ii) "in situ" hydrogel via the formation of a mutually interpenetrating network between the intestinal wall and the hydrogel. b) As-prepared hydrogels exhibit instant and strong mucoadhesion to the intestinal wall.

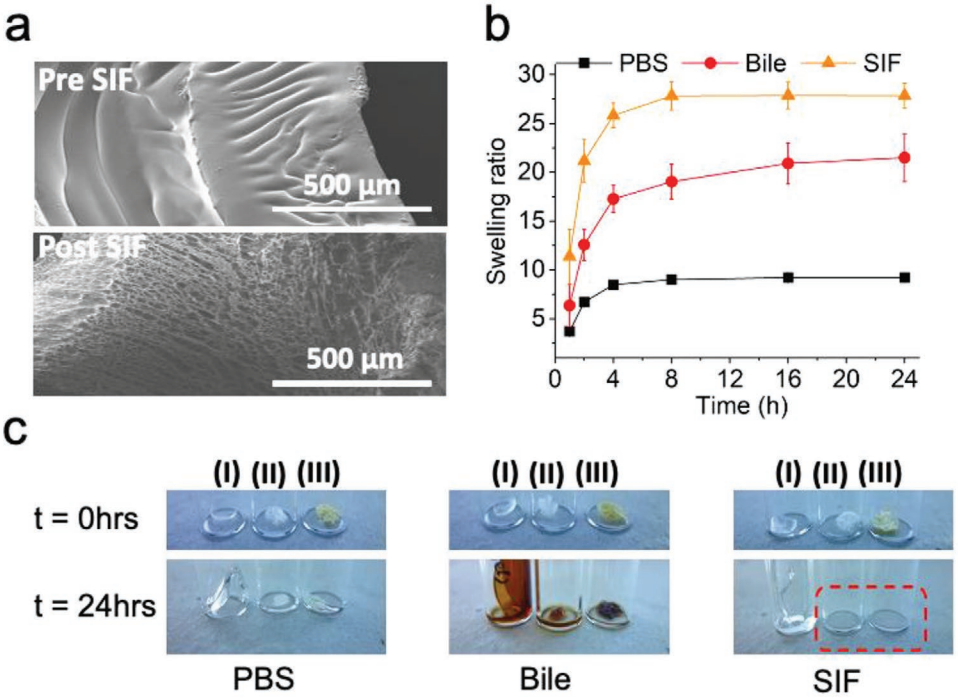

Figure 2. a) Scanning electron micrographs of the as prepared P(AAm-MA-AA) before interaction with SIF and after interaction with SIF. Estimated porosity of ≈59% post SIF. b) Swelling of the P(AAm-MA-AA) in different biological fluids. c) Stability of as prepared P(AAm-MA-AA) in PBS, bile and SIF compared to Tachosil: I) as prepared P(AAm-MA-AA), II) collagen backing of Tachosil, and III) fibrin adhesive layer of Tachosil. Red frame shows complete dissolution of Tachosil in SIF.

hydrogels: i) "ex situ": the as prepared P(AAm-MA-AA) hydrogel was applied directly to the serosa of fresh porcine small intestine, where the hydrogel was maintained in place solely by mucoadhesion (Figure 1b). ii) "in situ": the as prepared P(AAm-MA-AA) hydrogel was briefly incubated in an aqueous monomer mixture of identical composition to the hydrogel forming solution, prior to application to the intestinal tissue. Then, the soaked hydrogel was briefly irradiated in place by a low dose of UV, which allowed the monomers to form an interpenetrating network with the intestinal tissue and the hydrogel patch. The latter strategy aims to harness the synergistic effect between mucoadhesion and mechanical fixation to keep the gels anchored at the anastomotic site (vide infra).

Scanning electron microscopy (SEM) images (**Figure 2**a) of the as prepared hydrogels give insight into the physical characteristics of the gel network before (top) and after (bottom) exposure to intestinal fluid. These micrographs indicate an initially compact structure, which becomes highly porous following immersion in simulated intestinal fluid (SIF) (pore fraction of up to 59%, as quantified by image analysis [see Figure S4, Supporting Information]).

Figure 2b displays the swelling ratio between the mass at the swollen state and the mass of the as-prepared hydrogel, in various biological fluids as a function of time. Hydrogels reach a swelling plateau after 4 h of immersion, irrespectively of the biological fluid that they come in contact with. More specifically, swelling ratios increase from 7 in PBS to 27 in SIF (pH 6.8). This discretely different swelling behavior can be attributed to the slightly hydrophobic character[22] imparted to the hydrogel matrix by the methyl acrylate moieties. These force parts of the hydrogel network to phase separate in pure water[29] (see Figure S5, Supporting Information) while in solutions with a greater capacity for solubilizing hydrophobic molecules, such as SIF or bile,[30] poly(methyl-acrylate) segments favor interactions and thus allow for a greater swelling. This showcases the advantageous property of this material to quickly and preferentially absorb intestinal fluid compared to simple water solutions (PBS), which consequently establishes a first line of defense in the case of an anastomotic leak. The influence of the pH on the swelling of the adhesive was investigated by incubating the hydrogels in pH 2.0 (simulated gastric fluid[31]), pH 5.5 (ulcerative colitis[32]), and pH 8.0 (pancreatic effluents[33]) buffers (see Figure S6, Supporting Information). It was observed that the higher the pH the greater the swelling, with minimal swelling observed under gastric fluid conditions and maximal swelling under pancreatic fluid conditions. These results are in agreement with previously reported characteristics of poly(acrylic acid) containing hydrogels.[34,35] Furthermore, after contact with SIF, the hydrogel network appears to maintain its integrity (Figure 2c and Figure S3, Supporting Information). Clinically used Tachosil, on the other hand, not only changes texture but eventually completely dissolves over a 24 h period under the same conditions. This simple experiment directly shows the limitations of the currently clinically used fibrin-based patches for this scenario.

To quantitatively assess mechanical adhesion properties of the as prepared hydrogel, the formulations were tested using two different setups (**Figure 3**) and benchmarked against

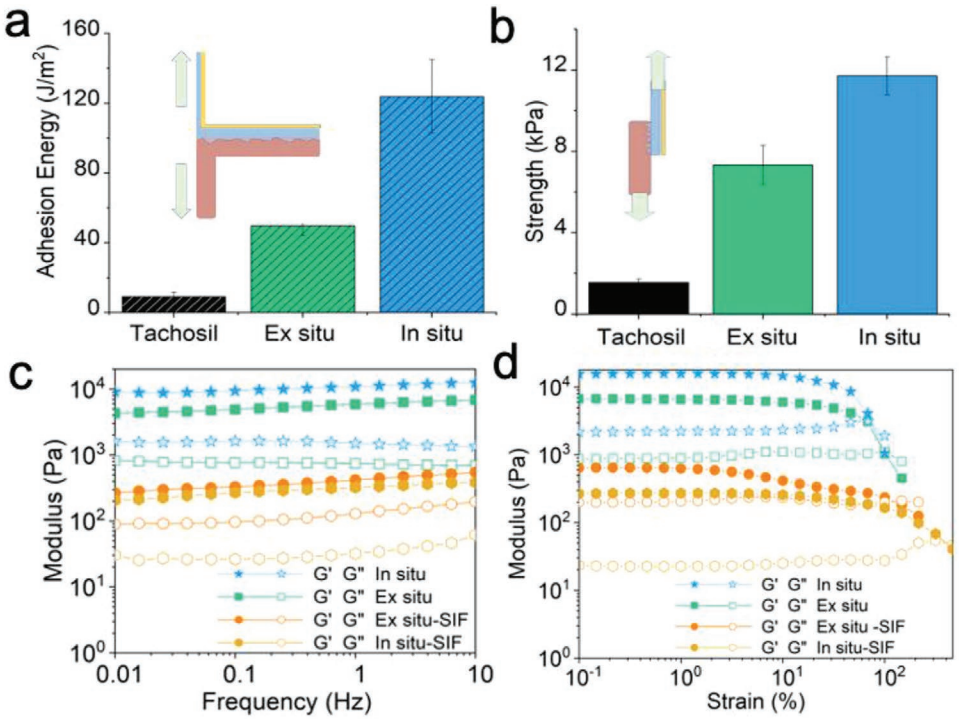

Figure 3. a) Adhesion energy in the T-peel and b) strength in the lap joint conformation of the P(AAm-MA-AA) ex situ and in situ formulations compared to Tachosil. Intestinal tissue is indicated in pale red, gel, and backing in blue and yellow. c,d) Rheological properties of as the synthesized gels after preparation and after 24 h contact with intestinal fluid.

commonly used Tachosil patches. The adhesion energy given by the T-peeling measurements (Figure 3a) and the adhesion strength by the lap shear measurements (Figure 3b) are shown for the three sample types. In both setups, Tachosil patches showed poor adhesion, which is in agreement with previous findings.[36] In the T-peel conformation, the ex situ P(AAm-MA-AA) hydrogel exhibited adhesion energy more than 5× higher than that of the surgical patch (50 versus 9 J m^{-2}), while the in situ applied hydrogels more than doubled the performance of the latter hydrogel (124 ± 21 J m^{-2}, 14× that of Tachosil). The contribution of the mutually interpenetrating network to the adhesion between the tissue and the hydrogel patch was investigated by varying the presence of acrylic acid moieties in both the patch and the mutually interpenetrating network (see Figure S7, Supporting Information). These findings suggest a synergistic character of mucoadhesion and mechanical fixation, with $E_{\text{in situ}} > E_{\text{ex situ}} + E_{\text{in situ*}}$ (where $E_{\text{in situ}} = 124$ J m^{-2}; $E_{\text{ex situ}} = 48$ J m^{-2} and $E_{\text{in situ*}} = 20$ J m^{-2} are the adhesion energies for in situ gels, ex situ gels, and AA-free in situ gels, respectively), indicating that both the penetrating network within the tissue as well as the hydrogel network itself are stronger when hydrogen bonding is present.[37] These results are in agreement with findings of Peppas et al.,[38–40] thus underlining the mechanisms of mucoadhesion of poly(acrylic acid) via the interdigitation of polymer chains with intestinal mucins. The work of Yang et al.[41] similarly showcases the improvements brought to adhesion by bond stitch topologies on various surfaces. It was concluded that strong hydrogen bonding originating from the presence of acrylic acid moieties is of paramount importance for the robust attachment, not only for the ex situ hydrogel patch but most importantly, also for the in situ one where attachment happens through the means of the mutually interpenetrating network.

This distinct difference between the ex situ and in situ P(AAm-MA-AA) hydrogels is further supported by the observation that in T-peel experiments, the serosa is stripped off the intestine in case of in situ, whereas it remains in place in the case of ex situ applied P(AAm-MA-AA) hydrogels (see Figure S8, Supporting Information). This macroscopic observation was confirmed by histological analysis of the intestinal samples after T-peel experiments. This further underlines the tissue attachment improvements brought by the formation of a mutually interpenetrating network between the tissue and the adhesive patch.

In lap shear measurements, the ex situ and in situ samples showed strengths of 7 and 12 kPa, respectively, both distinctively higher than that of the surgical patch Tachosil (2 kPa). The above results illustrate once more the advantageous performance of the cooperative sealing of mucoadhesive and mechanically fixed P(AAm-MA-AA) hydrogels compared to that of protein-based surgical products (e.g., Tachosil), toward the sealing and support of the anastomotic sites.

The mechanical properties of the hydrogel adhesives were further investigated using rheology. These investigations provide insight into the structural integrity of the hydrogel network and its limits, as well as the changes induced by the absorption of intestinal fluid. In Figure 3c, the moduli of the in and ex situ hydrogels, before and after immersion in intestinal fluid, are plotted as a function of frequency (oscillatory frequency-sweep measurements). While a slight increase in modulus can

be observed for the SIF exposed hydrogels, the moduli for all types of hydrogels remained rather constant throughout the frequency range of 0.01–10 Hz. This interval includes and exceeds the range of activity of the small intestine.[42] These results reveal the viscoelastic properties and long-term network stability of the hydrogels, which is crucial for the intended application. Expectedly, the in situ sample shows a storage modulus (G') double that of the ex situ hydrogel, due to its higher density of crosslinks and the presence of a network traversing interpenetrating network (Figure 3c). It is noteworthy that the exposure to SIF reduces the modulus of the hydrogels (G') from 750 to 380 Pa for the ex situ samples. Similarly, for the in situ hydrogels, a significant reduction of G' can be observed, passing from 1500 to 300 Pa. However, in spite of the modulus reduction induced by the absorption of the intestinal fluid, all the hydrogel networks remain intact, as revealed by the higher G' than G''.[43] This also indicates that the occurrence of swelling happens without compromising the network structures.

Such structural stability, when in contact with digestive SIF, was further demonstrated in Figure 3d, where the moduli of the hydrogels are plotted as a function of strain (oscillatory amplitude-sweep measurements[43]). The data display the broad linear viscoelastic regions of the as prepared samples, further affirming the high stability of the hydrogel network even after exposure to SIF (or bile and PBS see Figure S9a,b, Supporting Information). Moreover, while the moduli of all samples decreased after their incubation in SIF, their strains at the crossover point of G',G'' instead increase yielding network fracture strains exceeding 400% for in situ samples (see Figure S9c, Supporting Information). These data, indicate that the hydrogels can withstand a large deformation/strain, making them "fracture-proof" in the extent of the desired application (during anastomosis surgeries and post operation conjunct movement inside the body[44]), especially after exposure to SIF. Notably, these hydrogels possess comparable moduli to the surrounding tissues (muscle[45] 8–17 kPa, adipose tissue[46] ≈2 kPa).[47] This can avoid unwanted mechanical irritation that could be induced by mechanical mismatching between biomaterials and targeted tissues.

In **Figure 4**, the biocompatibility of the as-prepared hydrogels is overviewed and assessed via histology of fresh intestinal tissue sealed with adhesives, as well as indirect cytotoxicity. In order to characterize the cytotoxicity of the as-applied formulations, the lactate dehydrogenase (LDH) release of fibroblast cells was measured upon exposure to hydrogel-conditioned cell culture medium (Figure 4a). Following an evaluation method previously reported by Darnell et al.,[25] as-applied hydrogels were perfused with small quantities of cell medium simulating the gradual adaption of the materials during application. The perfusion was iterated up to four times and the medium was

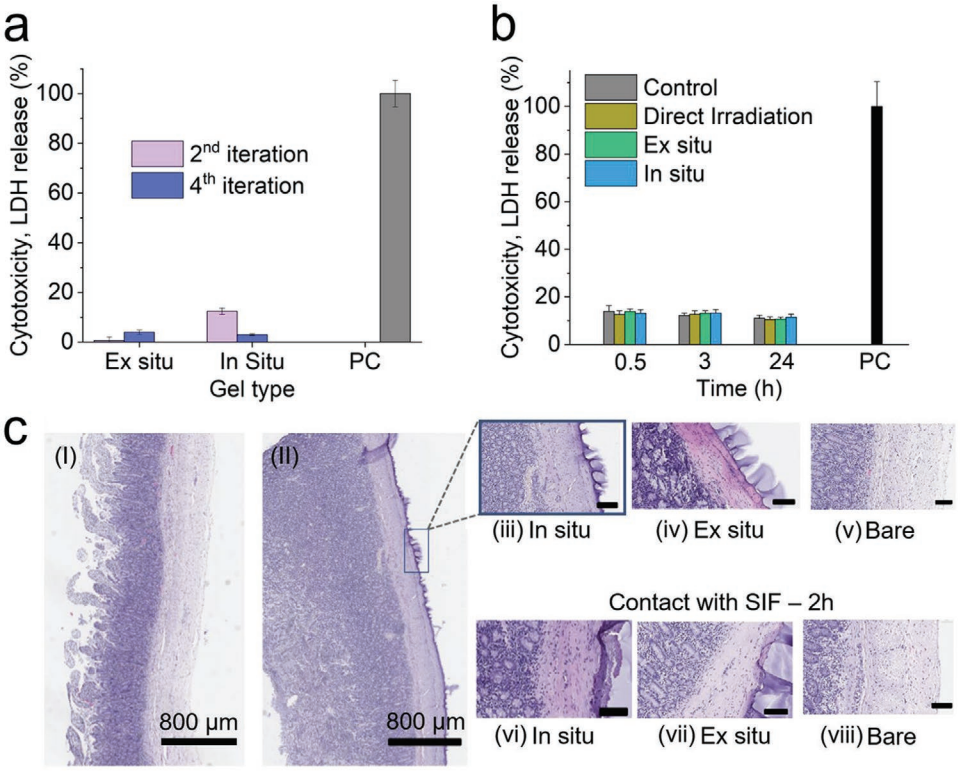

Figure 4. a) Lactate dehydrogenase (LDH) release cytotoxicity assay of fibroblasts treated with conditioned cell medium, as a function of perfusion iterations of 5 mL. b) LDH cytotoxicity assay of fibroblast cells after low dose UV irradiation, control samples represent shielded from irradiation cells and positive control (PC) the treatment of samples with Triton-X (full lysis). c) H&E stained biopsy cuts of: I) fresh bare porcine intestine, II) porcine intestine after application of an in situ P(AAm-MA-AA) hydrogel on the serosa. Images of the intestinal interface when in contact with the as prepared adhesives, upon application (top) and after 2 h of simulated, post surgery, static intestinal conditions in contact with SIF. Unassigned scale bars correspond to 100 µm.

thereafter added to the cells for LDH release assessment. The data suggests negligible cytotoxicity compared to the positive control already after the second iteration. This indicates a high biocompatibility of the as-prepared materials once perfused and adjusted to bodily conditions in good agreement with previous studies on alginate/polyacrylamide hydrogels.[25] Furthermore, Figure 4b shows the cell viability as a function of time after UV-irradiation. In order to emulate the conditions present during in situ hydrogel application, fibroblasts were exposed to the same UV light dose (9 J cm^{-2}, estimated for 180s) that was employed during the in situ application. Such UV light doses are used for other clinically relevant applications.[48,49] The cells were irradiated either directly or through a shielding layer of the prepared hydrogels. The cytolytic effect of UV irradiation, which was monitored via LDH release, appears to be minimal. In detail, an LDH release of ≈10% is reported, which is in the range of that of the control, shielded samples. The cytotoxicity levels remain unchanged after 24 h. These results along with the comparatively low dose of UV define the applicability window of the in situ applied hydrogel formulations and pave the way for robust sealants at the level of anastomosis sites.

Figure 4c shows the hematoxylin and eosin (H&E) staining of fresh porcine intestine once sealed with the prepared hydrogels and after 2 h of contact with SIF. This way, we sought to recreate the static and resting state of the intestinal tissue after surgery[50,51] and treatment with our sealants while avoiding tissue decomposition or digestion (see Figure S10, Supporting Information). More specifically, by comparing fresh-bare intestine to intestine that was sealed using an in situ hydrogel patch (Figure 4c-I,II), the firm interlocking of the in situ hydrogel with the tissue is made apparent and distinguishable by the purple coloration of the exterior lining of the intestinal serosa. Upon closer examination, both freshly applied in situ and ex situ samples (Figure 4c-iii,iv) are observed to firmly bond to the exterior of the intestinal wall, all while leaving the villous and serous structures intact and identical to the control (bare tissue - no sealant). Most notably in situ samples also show no apparent indication of deep penetration. Furthermore, after incubation with SIF we can conclude that neither in situ nor ex situ hydrogel samples (Figure 4c-vi,vii) cause observable damage to the intestinal serosa (compared to the control for the same time point) in the immediate or relatively extended amount of time following application. Last, in the same experiment Tachosil (see Figure S10, Supporting Information), as expected, exhibited no tissue alteration of any kind, leaving the structures of the intestine intact, similarly to the presented hydrogel adhesives, however with the distinct difference that no distinguishable feature related to its adhesive properties to tissue could be discerned.

Hydrogel penetration into the tissue was subsequently analyzed via histological staining and label-free Raman spectromicroscopy. **Figure 5**a shows histological sections for the ex and in situ formulations stained with methylene blue. Methylene blue has a high affinity for poly(acrylamide-co-acrylic acid) adsorbents[52] (see Figure S11, Supporting Information). It can be observed that the ex situ hydrogel is localized at the intestinal serosa interface. The in situ samples, on the other hand, exhibit a blue coloration of extended parts of the serosa, indicating the dimensions of the interpenetrating network into the tissue. Figures 5b and c show label-free Raman microscopy data processed by k-means cluster analysis.[53] Cluster maps (see Figure 5b) are in good agreement with the methylene blue-stained histological sections. The relative signal intensities of the methylene blue coloration and the polymer-rich cluster obtained from spectral analysis are shown as function of penetration depth in Figure 5c. These results indicate that the penetration of the in situ samples inside the tissue can be estimated at 26–30 µm. Ex situ samples are more localized and show a tissue overlap of 6–11 µm.

To evaluate the actual applicability of the hydrogel formulations as well as to assess the performance of these materials at sealing and controlling anastomotic leaks, a flow model (**Figure 6**a,b) and a stationary model (Figure 6c) were employed. In the flow model a piece of tubular porcine intestine was punctured using a circular 4 mm diameter biopsy punch and subsequently sealed with the prepared hydrogels or a size-equivalent Tachosil patch. The porcine intestine was then perfused with SIF at a flow rate of 1 mL min^{-1} and kept at 37 °C and 100% humidity.

The time before the first leakage incident is shown in Figure 6a. Most importantly, while the Tachosil patches leaked within the first 5 min, the ex situ hydrogel patch and the in situ patch remained attached and sealed for distinctively longer periods. In detail, the ex situ hydrogel patch exhibited partial detachment after 3 h and leakage after 5 h, while the in situ hydrogel remained attached and no leakage could be observed for the full duration of the experiment (24 h, after which even fully intact (control) porcine intestine started to leak).

Under the same conditions, bursting measurements indicating the maximum pressure the sealants could withstand are shown in Figure 6b. The burst pressures recorded are in line with the leakage sequence observed during the flow model, namely Tachosil bursts first followed by the ex situ samples and last by the in situ ones. The results further demonstrate the limitations of Tachosil as a support material for sutures in case of leaks of the anastomosis site. This is emphasized by the fact that Tachosil not only dissolves in intestinal fluid within hours (Figure 2c) but also exhibits bursting pressures (≈20 mm Hg) that barely coincide with the maximum pressure of a healthy intestinal tract.[54]

In order to simulate the pooling of intestinal fluid and to quantitatively assess the fluid leaking, a stationary model was developed. Figure 6c,d depicts the schematic representation and the results of the stationary model. Hydrogel samples were attached to a square piece of intestine, equipped with a 4 mm diameter hole. The intestine pieces were mounted on a cup, which was then filled with 10 g of SIF and gently agitated at 37 °C and 100% humidity to simulate natural intestinal movement and conditions. During this experiment, the mass of the leaked SIF was measured as a function of time and sample type. More specifically, in this configuration, which simulates harsh conditions of fluid pooling in the intestine, ≈9 g of the SIF in the Tachosil treated samples leaked after 0.5 h. Ex situ samples showed a deceleration of the leakage, with only 2 g of SIF leaking after 8 h. All ex situ patches, however, eventually detached, leading to a complete failure after 24 h. On the other hand, the in situ patches showed almost complete sealing up to 8 h. This amount is comparable to the control cups (no hole on

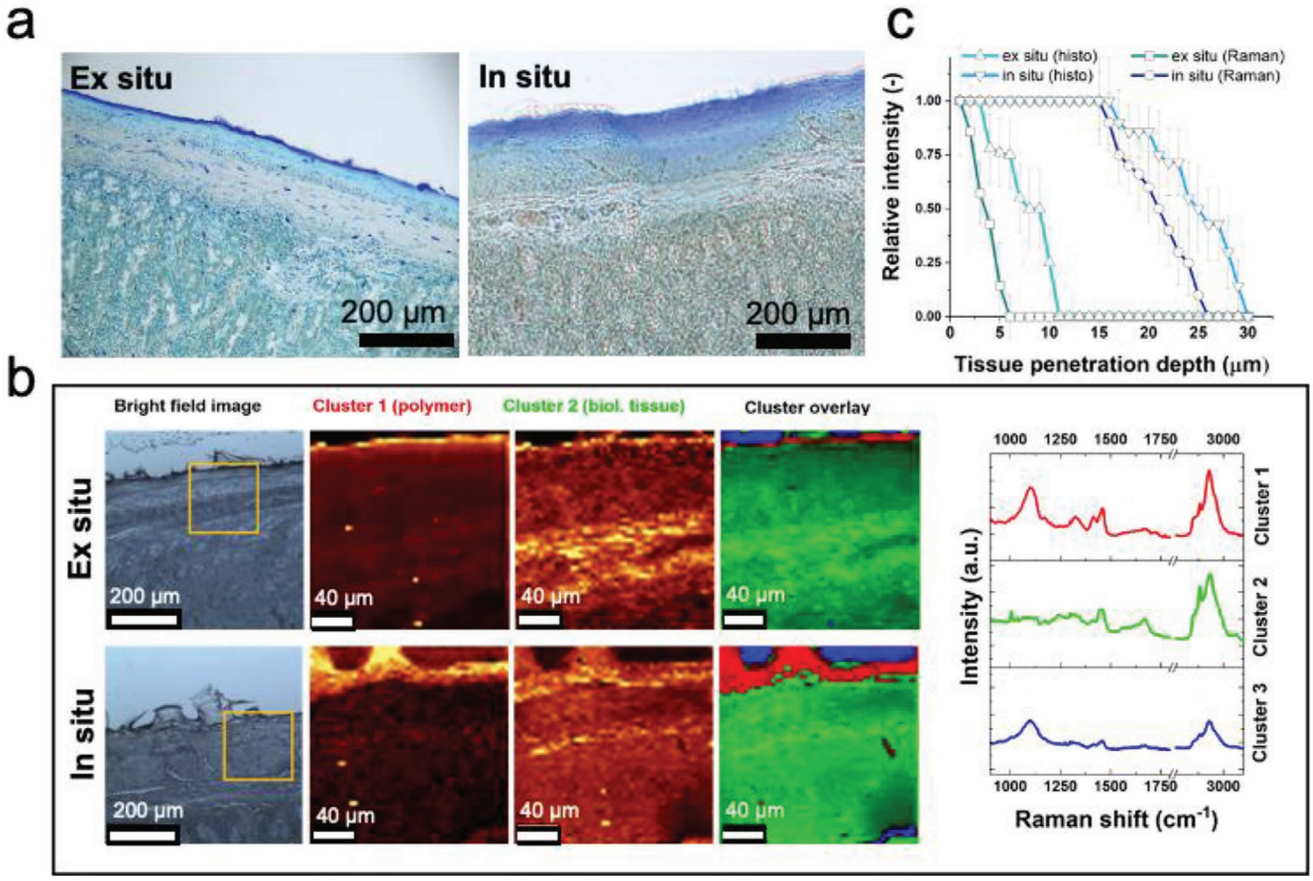

Figure 5. a) Histological tissue sections of porcine intestine with ex situ P(AAm-MA-AA) or in situ P(AAm-MA-AA) stained with methylene blue. b) Raman spectromicroscopy and corresponding k-means clustering maps and spectra of histological sections of ex situ and in situ sealed intestine (cluster 1 (P(AAm-MA-MA) polymer-rich), cluster 2 (biological tissue) and cluster 3 (substrate). c) Relative intensity of methylene blue staining and Raman spectromicroscopy as a function of penetration depth.

the tissue). Even after 24 h, the in situ treated samples, exhibited an accumulation of only 2 g, which is in the same range of the control experiment. The influence of the pH was also investigated with in situ samples (see Figure S12, Supporting Information). Fluids with pH 2 and 5.5 showed comparable performance to SIF (pH = 6.8), while a higher pH resulted in an early detachment. These results highlight the potential applicability of the prepared patches to scenarios with exposure to low to neutral pH fluids.

Taken together, the anastomosis sealant presented herein exhibited long-lasting and robust performance at countering and sealing anastomotic leaks in both static and dynamic testing conditions. Its tissue compatible mechanical anchoring and non-degradable mucoadhesive composition constitutes desirable and tailorable properties that not only guarantee performance but also set it apart from readily degradable[55] chitosan-based materials or purely mucoadhesive materials for the support of intestinal anastomosis sites.

3. Conclusion

In this study we prepared and evaluated the performance and behavior of novel mucoadhesive hydrogels, equipped with an interpenetrating network, mutually traversing tissue and patch, at the task of sealing anastomotic leaks. In contrast to the clinically used "gold standard" Tachosil patches, the prepared hydrogels maintained their mechanical integrity and were effective in preventing anastomotic leaking. In digestibility tests, the hydrogels maintained mechanical integrity while Tachosil completely dissolved. In stark contrast, the hydrogels prepared and evaluated during this study not only did not dissolve but also absorbed SIF leaks thanks to their chemical stability and swellable properties. Furthermore, both in situ and ex situ hydrogels exhibited mechanical properties compatible with the surrounding tissues as well as durability that could withstand anticipated stresses of the intraperitoneal cavity, even after exposure to simulated intestinal fluid. The incorporation of an interpenetrating hydrogel network which traverses the tissue and bridges hydrogel patch and intestinal wall together yielded an enhanced adhesion as well as a drastically decreased incidence of leakage in the flow and stationary setting, indicating an important desired characteristic of anastomotic sealants. The contributions to the synergistic performance enhancement were studied by varying the patch composition as well as the composition of its mutually interpenetrating network. The data acquired indicated that not only the desired properties of sealing but also remaining in place

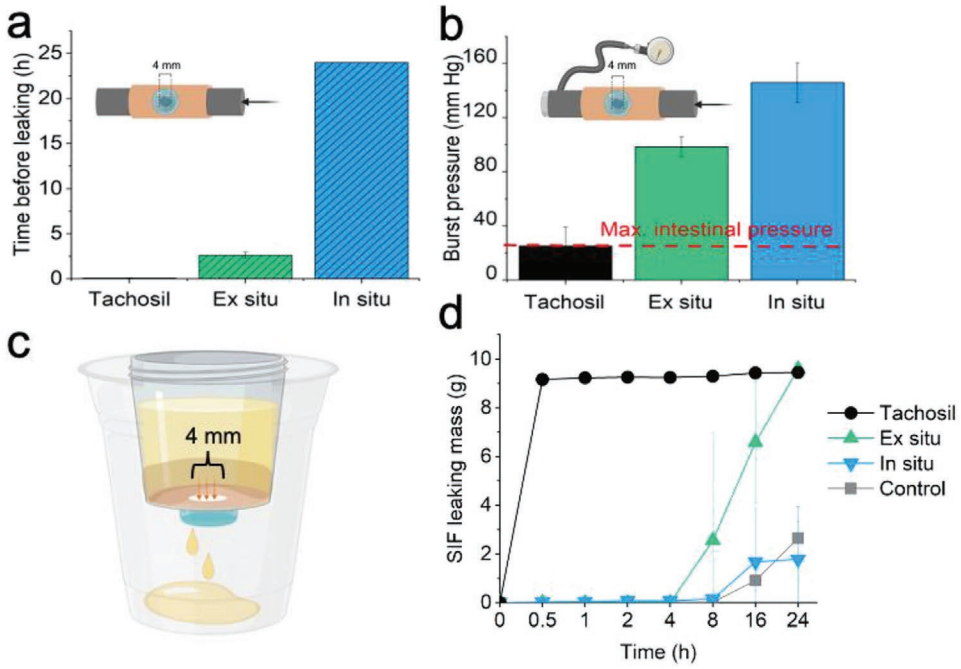

Figure 6. a) Ex vivo flow model simulating the flow of intestinal fluid at 1 mL min^{-1}, indicating leakage at discrete time points for the Tachosil patch, ex situ, and in situ hydrogels and b) burst pressure measurements for Tachosil patch, ex situ and in situ hydrogels. c) Illustration of stationary ex vivo model. d) Ex vivo stationary model simulating the pooling of intestinal fluid, indicating leaked mass of intestinal fluid over time.

for prolonged periods under the harsh intestinal conditions was attributable to the synergistic effect of mucoadhesion and mechanical fixation on the tissue. While the long term impact of the as prepared hydrogels needs to be further assessed, the use of acrylates as the main components of anastomosis sealants is proven advantageous, as their biocompatible and at the same time non-degradable properties can assure support to the sutured area, especially in cases of leakage of digestive fluids. Long-term toxicity and performance should be investigated in vivo, however, currently available rodent models of intestinal anastomotic leakage are poorly established and suffer from high variability.[56] Overall, this study underlined the importance of choosing sealants and suture supports based on their target tissue, as well as their desired and anticipated action. Furthermore, it provides evidence toward a non-negligible role of a robust mechanical support as a first-line treatment, in addition to the reported importance of healing when it comes to countering anastomotic leaks. Taken together, this work presents a blueprint for the development and application of high performance sealants designed and tailored for the treatment and prevention of anastomotic leaks.

4. Experimental Section

All materials were purchased from Sigma-Aldrich (Merck). AA and MA monomers were purified by passing them through a plug of basic alumina (Brockmann Grade I). Acrylamide, mBAA were used without further purification. Teflon molds for shaping hydrogels were prepared in-house with depths of 0.9 mm. Fresh small porcine intestine was obtained from Schlachtbetrieb St Gallen. The intestine was cleaned of its contents manually, divided into pieces and then stored at −20 °C. Intestine was preferably used fresh or thawed once and subsequently used for experiments.

Simulated Intestinal Fluid Preparation: Simulated intestinal fluid was prepared using lyophilized pancreatin powder (>8 USP) and a protocol from the united states pharmacopoeia (Test Solutions, United States Pharmacopeia 30, NF 25, 2007) as previously used in other studies.[57] In brief, (6.8 g, 50 mmol) monobasic potassium phosphate was dissolved in 250 mL Milli-Q water. To this solution, (77 mL 0.2 mol L^{-1}) sodium hydroxide solution and 500 mL Milli-Q water were added and mixed along with (10 g) pancreatin (from porcine pancreas, 8 USP units activity g^{-1}). The SIF/P suspension was adjusted to pH 6.8 with either 0.2 mol L^{-1} sodium hydroxide or 0.2 mol L^{-1} hydrochloric acid and diluted with water to 1000 mL.

Simulated Biological Fluids Used for pH Impact Studies: All simulated biological fluids described were used for the study of the influence of pH on the hydrogel network or sealing performance and as such were used without the inclusion of active enzymes. Simulated gastric fluid was made using the guidelines from the United States pharmacopoeia. More specifically, a 35 mM NaCl solution was prepared from distilled water. The solution was then adjusted to pH = 2.0 using 0.1 M HCl and used straight away. Simulated pancreatic fluid was prepared using simulated gastric fluid as a basis as reported by Paramera et al.[33] More specifically, 50 mL of the simulated fluid was prepared using a 35 mM NaCl solution as a background for dissolving 0.42 g of $NaHCO_3$, which was then adjusted to pH = 8.0. Ulcerative colitis simulated intestinal fluid, was prepared by using simulated intestinal fluid as previously described, but with the adjustment of the pH at 5.5 instead of 6.8 and the exclusion of pancreatin enzymes.

Hydrogel Preparation: In order to prepare the adhesive hydrogel patches, stock solutions of monomer mixes were prepared which were then assembled into master mixes.

First, a stock solution of AAm monomer was made by dissolving the powder in Milli-Q water at 20 wt%. A 2 wt% crosslinker was made by dissolution of (0.2 g, 1.3 mmol) mBAA dissolved in 9.8 g Milli-Q water. Both stock solutions were kept for a maximum 30 days stored at 0–4 °C. Photoinitiator stock solutions were made fresh before each

experiment and kept in the dark. More precisely, (9.5 mg, 42 µmol) 2-Hydroxy-4′-(2-hydroxyethoxy)-2-methylpropiophenone (Irgacure 2959) were dissolved in 2 mL Milli-Q water, by 20 min sonication. Previously cleaned monomers were then used to assemble the final hydrogel master mix. Typically, 6 mL of AAm monomer stock solution was mixed with 2.28 mL of AA, 1.25 mL of MA, 0.6 mL of photoinitiator Irgacure D-2959 solution and 61.7 µL of mBAA crosslinker stock solution. All constituents were vortexed in a 15 mL falcon tube. From the resulting mix 300 µL were spread to a Teflon round mold (diameter: 20 mm, depth: 1 mm). The mold was then put under a UVASPOT 400/T mercury lamp at a distance of 30 cm from the source. The light source was also equipped with a filter (H2) allowing the spectrum interval from 300 nm till the visible to reach the hydrogel mix. The P(AAm-MA-AA) hydrogel were obtained after 180 s irradiation. Hydrogel formulations excluding the presence of methyl acrylate were prepared by following the above-mentioned protocols of irradiation and molding. More specifically, for a 3 mL stock solution, 0.76 mL of AA, 2 mL of 20% AAm, 7.2 µL of mBAA 2% and 200 µL of 4.75 mg mL^{-1} Irgacure 2959 were mixed together. From the resulting solution 300 µL were placed in a Teflon mold and irradiated yielding a P(AAm-AA) gel.

Gel and Water Content Determination: Ex situ hydrogel samples were prepared as previously described. In situ simulated hydrogel samples were prepared by following the above described protocol for in situ hydrogel application but by irradiating the soaked samples on a Teflon surface instead of intestinal tissue. The resulting hydrogels were then immediately weighed and placed in a 1 L beaker filled with Milli-Q water and stirred at 400 rpm. The gels were then dialyzed against Milli-Q water over 24 h with the water background being exchanged four times over this period. Once dialyzed samples were flash frozen by incubation in liquid nitrogen for 20 min and then lyophilized using a CHRIST Alpha 3–4 LSCbasic (Adolph Kuhner AG, Switzerland) for 24 h. The samples masses were then once again recorded using a Mettler–Toledo analytic balance, AT201 (Mettler–Toledo (Schweiz) GmbH). Theoretical gel and water content was calculated by converting the volumes of pure monomer or monomer stock solutions to their equivalent mass using density or mass concentration respectively. The resulting monomer masses were summed yielding the theoretical gel content (assuming complete conversion). The corresponding water portions originating from the addition of monomer stock solutions were also summed to yield the theoretical water content. The theoretical ratio was calculated by dividing the theoretical water or gel mass with the total theoretical mass of the hydrogel (i.e., $M_{th.gel} + M_{th.water} = M_{th.tot}$).

$$\text{Gel content } \% = \frac{M_{aD}}{M_{aP}} \times 100 \tag{1}$$

$$\text{Water content } \% = 100 - \text{Gel content } \% \tag{2}$$

Where M_{aD} corresponds to the mass of the hydrogel after dialysis and lyophilization and M_{aP} to the mass of the hydrogel immediately after synthesis.

Scanning Electron Microscopy: Hydrogel samples that were either freshly prepared or swollen for 24 h in biological fluids were lyophilized for 24 h. Resulting pieces of these latter were mounted onto an SEM holder and coated with a (2.5 nm) layer of carbon via a Polaron Equipment (SEM coating Unit E5100, Kontron AG, Switzerland). Scanning electron microscope (SEM) imaging was performed on a Hitachi S-4800 (Hitachi High-Technologies, Canada) at an accelerating voltage of (2kV) and current flow of (10 µA). Images resulting from the above experiment were analyzed using ImageJ, by adjusting the contrast and setting a threshold in order to create a binary image. Once the binary image obtained the pore sizes were analyzed using particle analysis.

Fourier Transform Infrared: Infrared absorption spectra were measured using a Varian 640-IR spectrometer equipped with diamond attenuated total reflectance optics from previously vacuum dried hydrogels.

Nuclear Magnetic Resonance Spectroscopy: For NMR measurements, gels were freeze-dried, ball-milled into powder and dissolved in DMSO-d6 for solution-based NMR measurements.

Digestibility of Hydrogel Formulation: Hydrogel and Tachosil samples were respectively obtained from P(AAm-MA-AA) hydrogels and TACHOSIL Fibrin Sealant Patch using an (8 mm) biopsy punch. Each Tachosil sample was carefully separated into its two main components, fibrin and collagen sponge sides, which represent the active side (hemostatic) and non-active side of the Tachosil patch, respectively.[58] Samples, containing the as prepared P(AAm-MA-AA) hydrogel and Tachosil fibrin and collagen sponge sides were put into (4 mL) vials which were loaded with (3 mL) of PBS, bile or SIF were added respectively. Subsequently, all the vials were incubated on a platform shaker (Titramax 101, Heidolph, 200 rpm) at 37 °C. After 1 and 24 h, the liquid in each vial was removed using a syringe and injected back after observation. Pictures of all the vials were taken at the beginning, after 1 h and after 24 h.

Swelling Experiments: The relative swelling ratio R_{rel} is defined as,

$$R_{rel} = \frac{M_s}{M_i} \tag{3}$$

where M_S is the mass of the hydrogel sample after swelling for a given time point, M_i is the initial mass of the hydrogel sample. Initially, the as prepared hydrogels were transferred into vials. Then (3 mL) of PBS, bile or SIF ($N = 3$ for each fluid) were added respectively to investigate the dynamic hydrogel swelling in different physiological fluids. Finally, the vials were transferred onto a shaker (Titramax 101, Heidolph, 200 rpm) and incubated at 37 °C. The hydrogels were taken out and weighed after 1 h, 2 h, 4 h, 8 h, 16 h and 24 h swelling. The average relative swelling ratios in different simulated body fluids were obtained at different time points.

Ex Situ and In Situ Hydrogel Application: All hydrogel samples as well as Tachosil were applied on porcine small intestine serosa. For the ex situ samples, fresh hydrogels, prepared as previously described, were lifted from their molds using Teflon tweezers and parafilm. The hydrogel was then placed directly on the serosa of the intestine sample with attention to not include air bubbles at the interface with the tissue as well as to not lift the adhesive once in place. The hydrogel-intestine system was applied a weight of (1 kg) for 10 min on top of the parafilm backing. After that the weight and parafilm were removed and the sample system was used for subsequent experiments. In the case of in situ samples, hydrogels prepared as previously described were immersed for 10 min in the monomer master mix described previously, in a flat, closed petri dish. Hydrogels were flipped at intervals of 2 min in order to avoid curling of the gel and obtain a homogenous impregnation. At the same time, the intestine serosa was brought in contact with (150 µL) of monomer mix, at the area of application of the hydrogel (excluding the area of the (4 mm) hole). The swollen hydrogels were applied to the intestine making sure that no bubbles were trapped at the interface. The samples were then subjected to 180 s of low dose UV irradiation while placed on an aluminium foil containing a crushed ice bed, to mitigate tissue heating and drying. In the case of Tachosil, pieces of the surgical adhesive were cut in squares of (1.7 cm) side lengths, equaling the area of the developed hydrogels. The Tachosil patches were placed on the intestine serosa and a weight of 1 kg was applied to them for 10 min before using them for further experiments.

Adhesion Measurements: The adhesion strengths of the hydrogels on porcine small intestine were investigated following the procedures described in ASTM standard F 2256-05[59] (for the T peel test) and ASTM standard F 2255-05[60] (for the lap-shear test). Porcine small intestine was cut into pieces of 7 cm × 1.5 cm using a scalpel after being thawed at room temperature. In order to limit the deformation of the gel and tissue,[9] rigid transparent films (CG3720 color laser transparency film, 3M) used as backing layers, were cut to the size of P(AAm-MA-AA) hydrogels (5 cm × 1.8 cm × 0.1 cm) or intestine pieces and were attached to these latter with the use of a liquid superglue (Pattex Super Glue). The hydrogels were then applied to the intestine pieces as described earlier and the free ends of the hydrogel and the intestine piece were loaded to the instrument's clamps. The loading rate was kept constant at 250 mm min^{-1} and the standard force-strain curves were recorded. The T peel strength was calculated as the maximum plateau value of the ratio between the standard force and width of the sample.

Hydrogel Patch and Mutually Interpenetrating Network Formulation Studies on Adhesion: The inclusion or exclusion of acrylic acid moieties inside the patch or the mutually interpenetrating network was studied for its impact on adhesion. Hydrogels and mutually interpenetrating networks including acrylic acid moieties were prepared as earlier described. Hydrogels without acrylic acid moieties were prepared by excluding acrylic acid from the above described formulation. Methyl acrylate was also consequently removed from the formulations due to immiscibility with the remaining acrylamide solutions. More specifically, a 5 mL stock solution of 20 wt% acrylamide in Milli-Q water was prepared. To that was added 108 µL of mBAA crosslinker solution (2 wt%) and 500 µL of Irgacure 2959 solution (4.8 mg mL^{-1}). The solution was either loaded on a Teflon mold and irradiated for 3 min, yielding hydrogel patches without acrylic acid moieties or used to swell a previously made hydrogel patch in exactly the same manner as described previously for the in situ process. Adhesion energy was measured in the T-peel conformation as previously described.

Rheological Measurements: Dynamic shear oscillation measurements were used to characterize the viscoelastic properties of the hydrogel before and after swelling at 37 °C with SIF or other simulated bodily fluids such as PBS and bile. All the samples were fit to the rheometer (MCR 301, Anton Paar) receptacle size using a 25 mm Turnus Wad punch. Slippery samples due to swelling with biological fluids such as SIF were immobilized using sandpaper at the level of the Peltier and rotating plate. All measurements were carried out at 37 °C with the oscillatory strain sweep measurements being performed at constant frequency of 1 Hz while the oscillatory frequency sweep measurements were performed at a fixed constant strain of 1% over a frequency range of 0.01–10 Hz.

Adhesive-Intestinal Tissue Interaction Biopsies: After obtaining freshly collected porcine intestine from Schlachtbetrieb St Gallen in situ, ex situ and Tachosil adhesives were applied on the exterior surface of the fresh porcine intestine (not perforated). After application the treated intestine was sampled using an (8 mm) biopsy punch. The collected biopsies were immediately placed in a 4% formalin solution. After 24 h in formalin, the samples were separated from the bulk of the swollen hydrogel adhesive, leaving the interface intact, using surgical scissors. The same procedure was followed in the context of a stationary, post-surgery simulating experiment, where the as prepared samples were brought in contact with SIF at 37 °C, 100% humidity and light agitation. Intestinal tissue was subjected to both pancreatin rich and depleted SIF as a control. The collected biopsies were then sent to Sophistolab AG, Basel where they were block paraffinized, cut and stained using H&E. The samples were incubated for 5 min in Hematoxylin and 30 s in Eosin solutions. For preservation, the samples were dehydrated in steps (successively 70%, 80%, 90%, 96%, 100% EtOH, 2% isopropanol, 2× xylene, 2 min each) and mounted for subsequent storage. A ZEISS Primovert Microscope with an Axiocam 105 (Zeiss, Feldbach, Switzerland) color camera was used for image acquisition.

Methylene Blue Hydrogel Staining on Intestinal Tissue Biopsies: Histological sections were deparaffinized and rehydrated using an inverse xylene and decreasing EtOH concentration gradient steps. Following rehydration, samples were left in distilled water for 1 h for equilibration. The samples were then transferred to a 46 µM methylene blue solution for 15 min. The slides were then rinsed with distilled water and imaged directly after immobilized between a second microscope slide, keeping the samples in distilled water. The images were acquired using a A ZEISS Primovert Microscope with an Axiocam 105 (Zeiss, Feldbach, Switzerland) color camera was used for image acquisition. Image analysis using ImageJ was performed and by measuring the depth of the blue coloration at the interface of the tissue in at least 10 randomly selected locations on at least 3 independently acquired images.

Raman Microscopy on Sealed Intestinal Tissue: Raman measurements were performed as previously described.[53,61] More specifically, measurements were performed on deparaffinized histological sections. The measurements, were performed on a WITec alpha 300R confocal Raman microscope, equipped with a UHTS 300 Vis spectrometer and an Andor Newton EMCCD. A linearly polarized 532 nm laser was used for excitation. A 50× long distance objective was used (Zeiss, 50×/0.55 NA) and spectra were acquired with an integration time of 2 s with a step size of 2 µm and in maps of size (200 × 200 μm^2) starting at the outer surface of the intestinal sample. A laser intensity of 8 mW was used. The preprocessed (background-substracted and normalized) spectra were compressed using a three component PCA and fed to a k-means clustering analysis (Control Four Software, WITec). Image analysis was performed on cluster maps using ImageJ by measuring the depth of the polymer-rich cluster intensity at the interface of the tissue in at least ten different locations.

Serosa Investigation after Sealant Removal: Intestine samples were sealed with ex situ and in situ hydrogels, prepared as earlier described. The resulting samples were pulled off from the surface of the intestine (T-peel configuration) and samples of the tissue were collected after sealant pull off. The tissue samples were then fixed by immersion in a 4% formalin solution for 24 h (2 h at room temperature followed by 22 h at 0–4 °C). The resulting samples were dehydrated and embedded in paraffin using a Myr Spin Tissue Processor STP120 (Tarragona, Spain) for a total duration of 12 h for the dehydration and paraffin embedding. The paraffin embedded samples were then cut and put on microscope slides as described previously. H&E staining was performed on the acquired samples by first deparaffinizing and rehydrating the slides in inverse xylene and decreasing EtOH concentration gradients.

Perfused Medium Cytotoxicity Experiments: Perfused cell medium experiments were performed using a modified procedure inspired from Darnell et al.[25] More precisely, Normal Human Dermal Fibroblasts (NHDFs) (Sigma-Aldrich, Buchs, Switzerland), a non-cancerous human skin fibroblast cell line, was cultured under standard culture conditions at 37 °C with (5%) CO_2. Dulbecco's Modified Eagle's Medium–high glucose (DMEM) (#RNBG3787, Sigma, Buchs, Switzerland) supplemented with (10%) Fetal calf serum (FCS, Sigma-Aldrich, Buchs, Switzerland), (1%) L-Glutamine (Sigma-Aldrich, Buchs, Switzerland) and (1%) Penicillin-Streptomycin-Neomycin Solution (Sigma-Aldrich, Buchs, Switzerland) was used as full growth medium.

As applied hydrogel samples were placed inside (15 mL) falcon tubes and brought to swelling equilibrium by being incubated with (5 mL) of DMEM–high glucose supplemented with (10%) FCS for 4 h. The perfused hydrogel medium was then removed and collected marking the first perfusion iteration. The process was repeated four times. Per 96-plate well (4000 NHDF) cells were seeded in (100 µL) full growth medium and allowed to attach for at least 24 h. At time point 0 h, (100 µL) of perfused hydrogel supernatant or full growth medium as control was added respectively (total volume 200 µL). The plate was then incubated under standard culture conditions for 24 h. The cell viability was investigated through an LDH cytotoxicity assay using CytoTox 96 Non-radioactive Cytotoxicity assay (#G1780, Promega, Dübendorf, Switzerland.) and an ATP cell viability assay.

Irradiation Tolerance Experiments: In order to quantify the effects of UV irradiation on cells within the context of the application of the prepared hydrogels, (10 000) cells per 96 well plate were seeded and allowed to attach for 24 h. The culture medium was replaced by (180 µL) of fresh full growth NHDF medium. For irradiation on top of the cell containing plate another UV transparent 96 well plate of the same dimensions and loaded with the ex situ or monomer impregnated P(AAm-MA-AA) hydrogels was placed. No irradiation control samples were covered using a black tape. After a 180 s irradiation the cell containing plates were incubated at 37 °C and (5%) CO_2 for 0.5 h, 3 h and 24 h. The cell viability and cytotoxicity were studied on an LDH assay and an ATP cell viability assay.

Stationary Model: In order to evaluate the sealant properties of the hydrogels on tissue under the static conditions of the intestine, a cup-based setup was put in place (see Figure 4d). Briefly, a piece of intestine (7 cm) was cut along its length and spread on a piece of flat Teflon. The intestine was punctured with a hole simulating an opening at the level of the sutured anastomotic area, using a (4 mm) biopsy punch. Control samples were not equipped with a hole while hydrogels and surgical patches sealed the hole bearing intestine piece, using the previously described procedure. The sealed intestine was then mounted on a bottomless single-use polystyrene cup which and was kept in place by stapling its edges to the cup's wall. The intestine attached cup was subsequently placed on a second polypropylene cup of known mass. The system was then loaded with (10 mL) of freshly prepared simulated intestinal fluid or with the same quantity of simulated

gastric, pancreatic and ulcerative colitis fluid for pH variation experiments. All the samples were placed inside a styrofoam box equipped with water-soaked sponges to simulate the humidity of the intraperitoneal area and also loaded on a platform shaker operating at 40 rpm at 37 °C. The mass of the leaked SIF was then measured at discrete time intervals.

Flow Model: Roughly, (10 cm) long porcine small intestine pieces were equipped with a (4 mm) hole using a biopsy punch. The intestine pieces were then sealed by the as prepared hydrogels or the surgical patch Tachosil, as described previously. The sealed intestine was then hooked on a peristaltic pump setup allowing to perfuse the system with fresh 37 °C SIF at 1 mL min^{-1} from a (200 mL) reservoir (see Figure 6a). The samples were kept in a Styrofoam box equipped with symmetric holes, equally spaced for accommodating the tubular pieces of intestine. Funnels were placed under each sample, through the use of an appropriate exit hole for the collection of the leaked SIF. As in the static model, water-soaked sponges were added to the box in order to maintain 100% humidity. The time at which constant and repetitive leaking was observed was monitored and noted using a GoPro HERO4 for a period of 24 h.

Bursting Pressure: Bursting pressure was measured based on the previously described dynamic flow-model custom setup as shown in Figure 6b, with the only difference that flow was obstructed at the latter extremity of the intestine. The system was connected to a custom-built pressure sensor (30 021 430, Honeywell, Distrelec) and a syringe pump (NEMESYS, Cetoni GmbH, Germany). SIF was pumped through the system at a constant pumping speed of 10 mL min^{-1}. The maximum pressure reading was recorded as the burst pressure for each sample.

Supporting Information

Supporting Information is available from the Wiley Online Library or from the author.

Acknowledgements

The authors acknowledge Dr. Ignazio Tarantino for initial discussion of the ex vivo models and their clinical relevance, Apolline Anthis for her contributions to the initial composition and adhesive properties of the sealants and Henry Korhonen for his contributions to the initial design of the stationery and flow model. I.K.H. acknowledges funding from the Swiss National Science Foundation SNSF (Eccellenza grant no. 181290) and the vonTobel Foundation. The TOC, Figure 1 and Figure 6 were created using BioRender.com.

Conflict of Interest

A.H.C.A., M.T.M., and I.K.H. declare a conflict of interest in the form of inventorship on a patent application (EP21152240) related to a kit comprising an adhesive hydrogel and impregnating fluids. All other authors declare no competing interests.

Keywords

abdominal surgery, adhesive, hydrogel, sepsis, surgical glue

Received: August 21, 2020
Published online: February 1, 2021

[1] W. He, D. Goodkind, P. Kowal, *Int. Popul. Rep.* **2016**, *95*, 1.
[2] N. Hyman, T. L. Manchester, T. Osler, B. Burns, P. A. Cataldo, *Ann. Surg.* **2007**, *245*, 254.
[3] F. Goulder, *World J. Gastrointest. Surg.* **2012**, *4*, 208.
[4] K. Harada, S. Ida, Y. Baba, T. Ishimoto, K. Kosumi, R. Tokunaga, D. Izumi, M. Ohuchi, K. Nakamura, Y. Kiyozumi, Y. Imamura, M. Iwatsuki, S. Iwagami, Y. Miyamoto, Y. Sakamoto, N. Yoshida, M. Watanabe, H. Baba, *Dis. Esophagus* **2016**, *29*, 627.
[5] A. Sciuto, G. Merola, G. D. De Palma, M. Sodo, F. Pirozzi, U. M. Bracale, U. Bracale, *World J. Gastroenterol.* **2018**, *24*, 2247.
[6] T. Nordentoft, H.-C. Pommergaard, J. Rosenberg, M. P. Achiam, *Eur. Surg. Res.* **2015**, *54*, 1.
[7] A. H. Choudhuri, R. Uppal, *Ind. J. Crit. Care Med.* **2013**, *17*, 298.
[8] N. Annabi, Y.-N. Zhang, A. Assmann, E. S. Sani, G. Cheng, A. D. Lassaletta, A. Vegh, B. Dehghani, G. U. Ruiz-Esparza, X. Wang, S. Gangadharan, A. S. Weiss, A. Khademhosseini, *Sci. Transl. Med.* **2017**, *9*, eaai7466.
[9] J. Li, A. D. Celiz, J. Yang, Q. Yang, I. Wamala, W. Whyte, B. R. Seo, N. V. Vasilyev, J. J. Vlassak, Z. Suo, D. J. Mooney, *Science* **2017**, *357*, 378.
[10] Y. Otani, Y. Tabata, Y. Ikada, *Ann. Thorac. Surg.* **1999**, *67*, 922.
[11] F. Scognamiglio, A. Travan, I. Rustighi, P. Tarchi, S. Palmisano, E. Marsich, M. Borgogna, I. Donati, N. de Manzini, S. Paoletti, *J. Biomed. Mater. Res., B* **2016**, *104*, 626.
[12] E. D. van den Ende, P. W. H. E. Vriens, J. H. Allema, P. J. Breslau, *J. Pediatr. Surg.* **2004**, *39*, 1249.
[13] B. Mizrahi, C. F. Stefanescu, C. Yang, M. W. Lawlor, D. Ko, R. Langer, D. S. Kohane, *Acta Biomater.* **2011**, *7*, 3150.
[14] P. A. Leggat, D. R. Smith, U. Kedjarune, *ANZ J. Surg.* **2007**, *77*, 209.
[15] G. M. Taboada, K. Yang, M. J. N. Pereira, S. S. Liu, Y. Hu, J. M. Karp, N. Artzi, Y. Lee, *Nat. Rev. Mater.* **2020**, *5*, 310.
[16] A. Rickenbacher, S. Breitenstein, M. Lesurtel, A. Frilling, *Expert Opin. Biol. Ther.* **2009**, *9*, 897.
[17] S. J. Edwards, F. Crawford, M. H. van Velthoven, A. Berardi, G. Osei-Assibey, M. Bacelar, F. Salih, V. Wakefield, *Health Technol. Assess.* **2016**, *20*, 1.
[18] C. D. Liu, G. J. Glantz, E. H. Livingston, *Obes. Surg.* **2003**, *13*, 45.
[19] E. Fernández, D. López, E. López-Cabarcos, C. Mijangos, *Polymer* **2005**, *46*, 2211.
[20] J. Rosiak, K. Burozak, W. Pękala, *Radiat. Phys. Chem.* **1983**, *22*, 907.
[21] Y.-C. Nho, J.-S. Park, Y.-M. Lim, *Polymers* **2014**, *6*, 890.
[22] M. F. Refojo, F. L. Leong, *J. Biomed. Mater. Res.* **1981**, *15*, 497.
[23] S. Wu, L. Sun, J. Ma, K. Yang, Z. Liang, L. Zhang, Y. Zhang, *Talanta* **2011**, *83*, 1748.
[24] J. H. Ryu, H. J. Kim, K. Kim, G. Yoon, Y. Wang, G.-S. Choi, H. Lee, J. S. Park, *Adv. Funct. Mater.* **2019**, *29*, 1900495.
[25] M. C. Darnell, J.-Y. Sun, M. Mehta, C. Johnson, P. R. Arany, Z. Suo, D. J. Mooney, *Biomaterials* **2013**, *34*, 8042.
[26] E. M. Kampouris, A. G. Andreopoulos, *Biomaterials* **1989**, *10*, 206.
[27] BASF increases prices for acrylic monomers, Ink World, https://www.inkworldmagazine.com (accessed: April 2020).
[28] D. F. Eaton, in *Photochemistry, History and Commercial Applicç¸ations of Hexaarylbiimidazoles*, (Ed: R. Dessauer), Elsevier, Amsterdam **2006**, pp. 207–214.
[29] J. L. G. Ribelles, M. M. Pradas, G. G. Ferrer, N. P. Torres, V. P. Giménez, P. Pissis, A. Kyritsis, *J. Polym. Sci., Part B: Polym. Phys.* **1999**, *37*, 1587.
[30] A. J. Clulow, A. Parrow, A. Hawley, J. Khan, A. C. Pham, P. Larsson, C. A. S. Bergström, B. J. Boyd, *J. Phys. Chem. B* **2017**, *121*, 10869.
[31] L.-S. Wu, Z.-X. Li, Z.-C. Lu, M. Sun, K. Jamil, H. Lin, G.-Y. Wang, *Int. J. Food Prop.* **2015**, *18*, 43.
[32] A. G. Press, I. A. Hauptmann, L. Hauptmann, B. Fuchs, M. Fuchs, K. Ewe, G. Ramadori, *Aliment. Pharmacol. Ther.* **1998**, *12*, 673.
[33] E. I. Paramera, S. J. Konteles, V. T. Karathanos, *Food Chem.* **2011**, *125*, 913.
[34] S. Nesrinne, A. Djamel, *Arab. J. Chem.* **2017**, *10*, 539.
[35] J. E. Elliott, M. Macdonald, J. Nie, C. N. Bowman, *Polymer* **2004**, *45*, 1503.
[36] A. Toro, M. Mannino, G. Reale, I. D. Carlo, *J. Blood Med.* **2011**, *2*, 31.

[37] Q. Su, L. Duan, M. Zou, X. Chen, G. H. Gao, *Mater. Chem. Phys.* **2017**, *193*, 57.
[38] L. Achar, N. A. Peppas, *J. Controlled Release* **1994**, *31*, 271.
[39] N. A. Peppas, Y. Huang, *Adv. Drug Delivery Rev.* **2004**, *56*, 1675.
[40] E. Jabbari, N. Wisniewski, N. A. Peppas, *J. Controlled Release* **1993**, *26*, 99.
[41] J. Yang, R. Bai, J. Li, C. Yang, X. Yao, Q. Liu, J. J. Vlassak, D. J. Mooney, Z. Suo, *ACS Appl. Mater. Interfaces* **2019**, *11*, 24802.
[42] E. P. Widmaier, H. Raff, K. T. Strang, A. J. Vander, *Vander's Human Physiology : The Mechanisms of Body Function*, McGraw-Hill, Boston, MA **2008**.
[43] D. K. Baby, in *Rheology of Polymer Blends and Nanocomposites*, (Eds: S. Thomas, C. Sarathchandran, N. Chandran), Elsevier, Amsterdam **2020**, pp. 193–204.
[44] W. E. Brant, C. A. Helms, *Fundamentals of Diagnostic Radiology*, Lippincott Williams & Wilkins, Philadelphia, PA **2007**.
[45] J. Liu, H. Zheng, P. Poh, H.-G. Machens, A. Schilling, *Int. J. Mol. Sci.* **2015**, *16*, 15997.
[46] I. Van Nieuwenhove, L. Tytgat, M. Ryx, P. Blondeel, F. Stillaert, H. Thienpont, H. Ottevaere, P. Dubruel, S. Van Vlierberghe, *Acta Biomater.* **2017**, *63*, 37.
[47] L. A. Johnson, E. S. Rodansky, K. L. Sauder, J. C. Horowitz, J. D. Mih, D. J. Tschumperlin, P. D. Higgins, *Inflammatory Bowel Dis.* **2013**, *19*, 891.
[48] X. Chen, M. Yang, Y. Cheng, G. J. Liu, M. Zhang, *Cochrane Database Syst. Rev.* **2013**, *10*, CD009481.
[49] E. Adışen, V. Tektaş, F. Erduran, Ö. Erdem, M. A. Gürer, *Dermatology* **2017**, *233*, 192.
[50] K. F. Güenaga, S. a. S. Lustosa, S. S. Saad, H. Saconato, D. Matos, *Cochrane Database Syst. Rev.* **2007**, *1*, CD004647.
[51] A. L. Lightner, J. H. Pemberton, *Clin. Colon Rectal Surg.* **2017**, *30*, 178.
[52] Q. Lv, Y. Shen, Y. Qiu, M. Wu, L. Wang, *J. Appl. Polym. Sci.* **2020**, *137*, 49322.
[53] M. S. Bergholt, J.-P. St-Pierre, G. S. Offeddu, P. A. Parmar, M. B. Albro, J. L. Puetzer, M. L. Oyen, M. M. Stevens, *ACS Cent. Sci.* **2016**, *2*, 885.
[54] P. R. Kvietys, D. N. Granger, *Ann. N. Y. Acad. Sci.* **2010**, *1207*, E29.
[55] E. L. McConnell, S. Murdan, A. W. Basit, *J. Pharm. Sci.* **2008**, *97*, 3820.
[56] J. W. A. M. Bosmans, M. Moossdorff, M. Al-Taher, L. van Beek, J. P. M. Derikx, N. D. Bouvy, *Int. J. Colorectal Dis.* **2016**, *31*, 1021.
[57] N. Kaur, A. Narang, A. K. Bansal, *Eur. J. Pharm. Biopharm.* **2018**, *129*, 222.
[58] TACHOSIL safety and utilization review, FDA, https://www.fda.gov/media/130845 (accessed: August 2020).
[59] ASTM F2256-05(2015), Standard Test Method for Strength Properties of Tissue Adhesives in T-Peel by Tension Loading, ASTM International, West Conshohocken, PA **2015**.
[60] ASTM F2255-05(2015), Standard Test Method for Strength Properties of Tissue Adhesives in Lap-Shear by Tension Loading, ASTM International, West Conshohocken, PA **2015**.
[61] M. T. Matter, J.-H. Li, I. Lese, C. Schreiner, L. Bernard, O. Scholder, J. Hubeli, K. Keevend, E. Tsolaki, E. Bertero, S. Bertazzo, R. Zboray, R. Olariu, M. A. Constantinescu, R. Figi, I. K. Herrmann, *Adv. Sci.* **2020**, *7*, 2000912.